

# ChemComm

Accepted Manuscript



This is an *Accepted Manuscript*, which has been through the Royal Society of Chemistry peer review process and has been accepted for publication.

*Accepted Manuscripts* are published online shortly after acceptance, before technical editing, formatting and proof reading. Using this free service, authors can make their results available to the community, in citable form, before we publish the edited article. We will replace this *Accepted Manuscript* with the edited and formatted *Advance Article* as soon as it is available.

You can find more information about *Accepted Manuscripts* in the [Information for Authors](#).

Please note that technical editing may introduce minor changes to the text and/or graphics, which may alter content. The journal's standard [Terms & Conditions](#) and the [Ethical guidelines](#) still apply. In no event shall the Royal Society of Chemistry be held responsible for any errors or omissions in this *Accepted Manuscript* or any consequences arising from the use of any information it contains.

Cite this: DOI: 10.1039/c0xx00000x

www.rsc.org/xxxxxx

ARTICLE TYPE

# Methoxy Functionalisation: Exerting Synthetic Control of the Supramolecular and Electronic Structure of Nitrogen-doped nanographenes

Lankani P. Wijesinghe,<sup>a,b†</sup> Buddhie S. Lankage,<sup>a,b†</sup> Gearóid M. Ó Máille,<sup>a,b</sup> Sarath D. Perera,<sup>a,b,c</sup> Deanne Nolan,<sup>a,b</sup> Longsheng Wang,<sup>a,b</sup> Sylvia M. Draper<sup>a,b\*</sup>

Received (in XXX, XXX) Xth XXXXXXXXX 20XX, Accepted Xth XXXXXXXXX 20XX

DOI: 10.1039/b000000x

**Abstract:** We describe a series of functionalized N-containing heterosuperbenzenes, created with a view to investigating the strategic role of methoxy substituents in (i) promoting cyclodehydrogenation and (ii) tuning the electronic properties and (iii) the supramolecular order in the resultant fused products.

The dominance of inorganic semiconductors in the manufacture of optoelectronic devices and field effect transistors is gradually being undermined by the emergence of functional organic materials.<sup>1-3</sup> Although electron mobility remains a challenge, these represent lightweight, flexible alternatives that are more readily processed using solution-based methods. Within this arena, the opportunities proffered by the exceptional electronic and physical properties of graphene and its derivatives are undeniable.<sup>4-6</sup>

As many aspects in the formation of large graphitic sheets are difficult to control, synthetic chemists have pioneered routes to nanographenes with impressive and varying dimensions, and an array of peripheral substituents.<sup>7-10</sup> Dependent on the latter are a range of material characteristics e.g. the nature of the  $\pi$ - $\pi$  interactions, HOMO-LUMO gaps and film-forming capabilities.<sup>11-14</sup> The ability to manufacture graphene systems to such specificity is notably absent in exfoliation<sup>15</sup>/epitaxial growth<sup>16</sup> processes, and this makes the further development of bottom-up synthetic methodologies for the formation of next-generation and heteroatom-containing graphenes all the more important.<sup>10, 17</sup>

Oxidative cyclodehydrogenation is a key step in the chemical formation of planarised ring systems. All-carbon systems cyclise rapidly, while heteroatom-containing polyphenylenes appear to adopt a more complex mechanism for ring closure, e.g. both partially and fully fused species tend to be generated in a single reaction.<sup>18-20</sup> Electron donating substituents both direct and promote CC bond formation under cyclodehydrogenation conditions.<sup>21, 22</sup>

Tuning the intramolecular properties of graphenes is one step in the search for technology-enabling materials. Also essential is the ability to exert some supramolecular control of structure. Disc-like molecules tend to aggregate in columnar  $\pi$ - $\pi$  stacks which can be either enhanced or perturbed by peripheral units e.g.

long chain alkyl substituted hexaperihexabenzocoronenes frequently exhibit liquid crystalline behaviour,<sup>2</sup> whereas their iodo- or *tert*-butyl- functionalised derivatives give rise to Bernal-stacked crystalline dimers.<sup>23</sup>

This work reveals how the combination of heteroatom doping (as pioneered by Draper *et al.*),<sup>17, 24-26</sup> with H-bonding peripheral substituents, can unlock some exciting new applications for nanographene materials by controlling the outcome of the synthetic process and the HOMO-LUMO gaps and intermolecular order of the end-products.

The synthetic methods used to form the precursor polyphenylenes were modifications of published routes involving cyclopentadienones (generated *via* two-fold Knoevenagel condensations) and their subsequent [2+4] Diels Alder cycloadditions with either a di-pyrimidyl (4N)<sup>17</sup> or monopyrimidyl (2N) acetylene (see Supporting Information (SI)). These reactions resulted in the formation of the novel methoxy-substituted N-doped polyphenylenes **1**, **3**, and **5** which were subsequently subjected to oxidative cyclodehydrogenation. *Via* unpublished work, the authors have established that the analogous 2N *tert*-butyl-containing systems (lacking methoxy substituents) would not fully cyclise under similar conditions.

The strategic positioning of peripheral methoxy groups is therefore key to generating this new series of nanographenes. The FeCl<sub>3</sub>-mediated oxidative cyclodehydrogenation of the '*para*'-methoxylated **1** gave the new nitrogen heterosuperbenzene **2** (Scheme 1(a)).

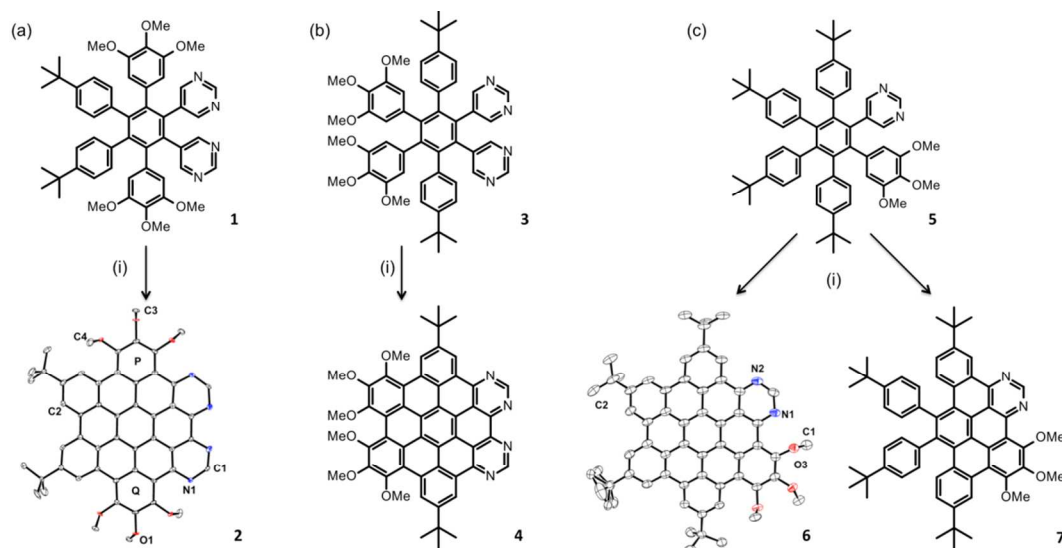
Under the same conditions, reaction of **3** gave rise to the '*ortho*'-methoxylated **4** (Scheme 1(b)), which proved challenging to purify due to the presence of a trace of the 5/6-cyclised product. Two products were isolated from the reaction of **5** under these conditions: the fully fused **6** (40 % yield) and the co-synthesised half-cyclised **7** (10 % yield). The products were all purified *via* column chromatography and on preparative plate thin layer chromatography. Full synthetic details and NMR analysis and discussion are available in the SI.

**2** and **6** crystallise in the monoclinic P2<sub>1</sub>/c space group, with four molecules in the unit cell. Compound **4** unfortunately did not provide suitable crystals. Both show some distortion of the planar core due to steric congestion. In **2**, for example, ring P is bent by 11.6° with respect to the central phenyl ring (Scheme 1 (a)). In

Cite this: DOI: 10.1039/c0xx00000x

www.rsc.org/xxxxxx

## ARTICLE TYPE



**Scheme 1** The synthetic routes to 4N (a and b) and 2N (c) methoxy functionalized polyaromatic systems (i)  $\text{CH}_2\text{Cl}_2$ ,  $\text{FeCl}_3$  (30 eq. in  $\text{CH}_3\text{NO}_2$ ), 4 h, (c) 24h; Yields (a) **1**: 88%; **2**: 53% (b) **3**: 82%; **4**: 35% (c) **5**: 54%; **6**: 40%; **7**: 10%. Crystal structures are shown for **2** and **6** (hydrogens removed for clarity, thermal ellipsoids shown at 50 % probability. **6** shows a disordered tert-butyl group). Atomic and ring labelling is to aid the crystallographic discussion (vide infra).

each of the rings P and Q, two adjacent methoxy substituents point in the same direction (either above or below the central plane). The methoxy groups exist in a ‘two up, one down’ arrangement on each ring. This has a profound effect on the packing, resulting in offset head-to-tail dimers (AB) in a columnar stack (Figure 1).

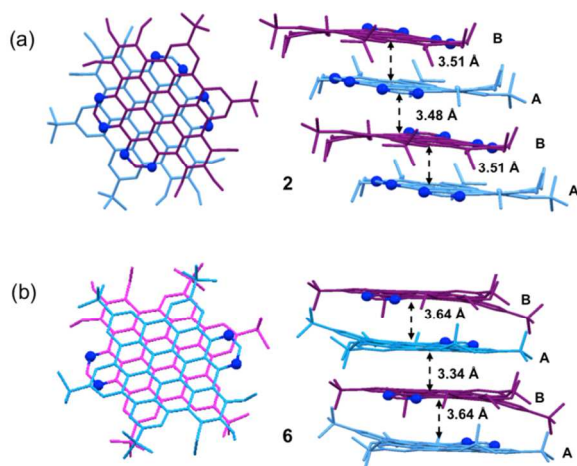


**Fig. 1** X-Ray crystal structures of **2** and **6**. (left) Head-to-tail packing arrangement and (right) side-view of the dimeric packing arrangement of (a) **2** and (b) **6**

The  $\pi \cdots \pi$  stacking is reflected in the short intradimer distance (A-B is 3.48 Å), while the interdimer distance is longer (AB-AB is 3.51 Å, see Figure 1(a), right). The AB dimers are not arranged in typical Bernal packing, but are offset by 1.25 Å. In addition to the

$\pi \cdots \pi$  interactions, the dimers are held together by intermolecular hydrogen bonds between a methoxy-based methyl H and a methoxy O and a pyrimidyl N atom, ( $\text{O1} \cdots \text{H-C4}$  (3.53 Å, 160.06°) and  $\text{N1} \cdots \text{H-C3}$  (3.50 Å, 149.43°)).

The crystal structure of **6** is shown in Scheme 1(c) and in Figure 1(b). The methoxy groups arrange themselves in a manner analogous to that observed in **2**. Intramolecular H-bonding is observed ( $\text{N1} \cdots \text{H-C1}$  (3.072 Å) with a donor acceptor bond angle of 112.65°). **6** adopts a similar packing arrangement to **2**, however the intradimer  $\pi \cdots \pi$  distances are shorter (3.45 Å) with a larger offset (3.12 Å) and the distances between the dimers are slightly longer (3.64 Å) (see Figure 1(b)). In **2**, the methoxy substituted rings of the dimeric molecules are above each other whereas in **6** they avoid each other.

Figure 2(a) compares the absorption spectra of compounds **2**, **4**, **6** and **7** in toluene. Being the least aromatic compound in the series, **7** displays both the most hypsochromically shifted  $\lambda_{\text{max}}$  (305 nm) and the broadest absorptions. The remaining members of the series display a prominent absorption at  $\lambda_{\text{max}}$  355 nm, as is typical of other benzenoids<sup>11</sup> and fully fused N-HSB.<sup>17</sup> The  $\lambda_{\text{max}}$  absorption in each case is relatively insensitive to both substitution and solvent polarity, and is characteristic of the  $\beta$  band described by Clar.<sup>27</sup> While  $\beta$  bands are generally  $\pi\text{-}\pi^*$  in character, a marked hypochromic shift in acidic medium points to some underlying  $n\text{-}\pi^*$  contribution, as also seen in N-HSB.<sup>17</sup> p-Bands, associated with electron relocalisation in the excited state, are also evident in the fully-fused systems **2**, **4**, and **6**. They appear to be only moderately affected by substituent effects, being consistently centred around  $\lambda \approx 400$  nm. This, coupled with a small hypochromic shift for this band in acidic medium (and the

absorption's absence in the parent hydrocarbon) leads us to conclude that this band has significant  $n-\pi^*$  character. The lowest energy absorptions observed in each fully fused compound are the purely electronic, symmetry forbidden  $\alpha$  (0-0) bands ( $\lambda = 470$  – 500 nm). The low symmetry (approximate  $C_{2v}$  or less) of **2**, **4** and **6** results in the enhanced intensity of these bands.<sup>28</sup> From the transitions' energies we calculate HOMO-LUMO gaps of 2.48 eV for (4N) **2** and **4**, and 2.60 eV for (2N) **6**. This is reminiscent of the smaller band gap found in N-containing systems of higher N-doping by Bronner *et al.*<sup>29</sup>

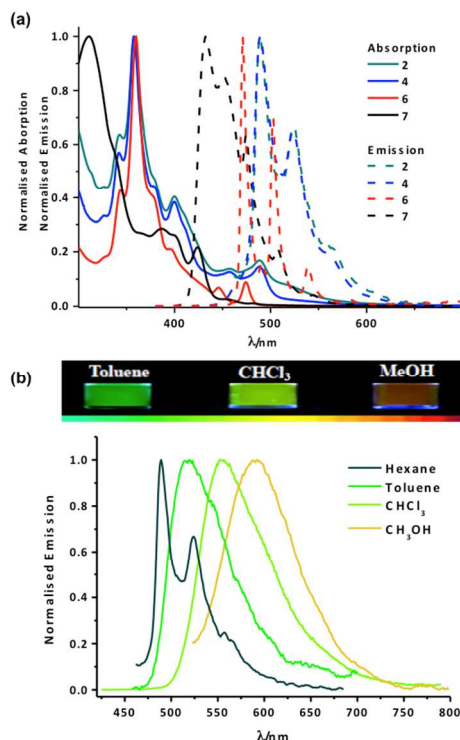


**Fig. 2** (a) Normalised room temperature UV-Vis absorption (toluene) and emission (hexane) spectra of **2**, **4**, **6**, and **7**. (b) Normalised emission and photographic representation of the solvatochromic response of **4**.

The compounds are intensely fluorescent, and display prominent vibrational progressions in non-polar solvents. The most hypsochromically-shifted feature of the emission overlaps with the  $\alpha$  absorption band, indicating minimal geometry change in the excited state. The partially unfused nature of **7** leads to the compound displaying the most blue-shifted emission of the series, at  $\lambda_{em}$  432 nm. While the molecule is not completely rigid, vibrational progressions of *ca.* 1200  $cm^{-1}$  are observed in hexane. The compound also exhibits a short lifetime and the lowest emission quantum yield in the series (21 %, see Table S1 in SI). Its fully fused counterpart (**6**) is red shifted due to its more aromatic nature ( $\lambda_{em} = 470$  nm,  $\tau = 8.3$  ns). Along with the other fully-fused compounds in the series, its rigidity results in prominent vibrational spacings of approximately 1350  $cm^{-1}$ . Fusion has also resulted in an increased emission quantum yield of 53 % for the fully fused compound (**6**) and 32 % for the 4N compound (**2**). Considering the donor-acceptor nature of these systems, it can be surmised that the initial locally-excited state can give rise to an intramolecular charge-transfer (ICT) state

which is highly stabilised by polar solvents. This rationalises both the dramatic solvatochromic shifts observed, and the broadness of the emissions in methanol (Figure 2(b) and S6 in SI). Due to their higher inherent dipole moment, **2** and **4** give a far greater solvatochromic shift than **6** (3500  $cm^{-1}$  and 3400  $cm^{-1}$  respectively, compared with 1578  $cm^{-1}$ ). The position of the MeO groups does not appear to affect the magnitude of the solvatochromic shift. Low temperature measurements were carried out on the compounds in 77 K butyronitrile glass. Each showed a moderate rigidochromic shift and a concomitant increase in emission lifetimes, as expected in rigid media (see Table S1 in SI).

In order to gain further insight into the spectroscopic behaviour observed, cyclic voltammetry was employed to investigate the specific effects of  $-OMe$  functionalisation and N-doping on the systems' HOMO and LUMO levels. Each planarised compound shows a single irreversible oxidation process under positive potential. Compound **2** is the most readily oxidised, due to its six  $-OMe$  groups increasing the HOMO energy ( $E_p = 0.65$  V vs.  $Fc/Fc^+$ ) (see Table S1 in SI). The lesser degree of  $-OMe$  functionalisation in **6** results in a more stabilised HOMO, giving a less facile oxidation ( $E_p = 0.78$  V). Although **7** also bears three  $-OMe$  groups, it presents the most difficult oxidation due to its lower aromaticity, which serves to further stabilise the HOMO ( $E_p = 0.86$  V). The reduction potentials are principally governed by the electron-withdrawing N-atoms present: **6** (2N) displays a reversible reduction wave at  $E_{1/2} -2.02$  V, while **2** (4N) is shifted to  $E_{1/2} -1.62$  V due to its LUMO-destabilising four N-atoms. The hardest reduction is that of **7**, arising from its reduced aromaticity (which imparts a relatively destabilised LUMO). While low yields precluded the study of the electrochemical characteristics of **4**, these data correspond well with that of the similar *tert*-butyl N-HSB.<sup>18</sup> In essence, these results show the fine-tuning of the available band gaps in these materials.

We have synthesised a novel set of methoxy-substituted 2N and 4N-containing heterosuperbenzenes. CC bond formation and ring closure were promoted by incorporating strategically-placed and electron-donating methoxy substituents in the precursor polyphenylenes. Methoxy substitution has profoundly affected the supramolecular order observed in the crystalline nanographenes. The propensity for methoxy groups to engage in weak H-bonding appears to assist the molecules to orient in a head-to-tail arrangement within columnar  $\pi-\pi$  stacks. The systems' HOMO-LUMO gap has been rendered smaller by the HOMO destabilising MeO groups and the LUMO stabilising N-atoms. Importantly, this means that the electronic properties are under the control of the dopants and the peripheral units. In the search for small band gap materials this may negate the need to greatly extend the dimensions of the aromatic platform. Both band gap and inter-layer control are immensely important in investigations to broaden the application of nanographenes. This work points to the ability to control both parameters simply *via* chemical means.

## Notes and references

<sup>a</sup> School of Chemistry, Trinity College, College Green, Dublin 2, Ireland. E-mail: smdraper@tcd.ie; Fax: +353 1 617 2826; Tel: +353 1 896 2026

<sup>b</sup> Centre for Research on Adaptive Nanostructures and Nanodevices (CRANN), Trinity College Dublin, Dublin 2, Ireland

<sup>c</sup> Chemistry Department, The Open University of Sri Lanka, Nugegoda, Sri Lanka

<sup>†</sup> These authors contributed equally to the experimental data presented  
<sup>‡</sup> The terms *para* and *ortho* are used here to describe the positioning of the 3,4,5-trimethoxybenzene units with regard to the central ring.

We thank Drs. J. O'Brien and M. R  ther for spectroscopic and technical assistance. We thank the Science Foundation Ireland for financial support (SFI 10/IN.1/12974, SFI 09/RFP/MTR2366). LPW wishes to thank Trinity 1252 postgraduate award.

Electronic Supplementary Information (ESI) available: experimental procedures and the characterization data for all new compounds, S1- S6. Single crystal X-ray data are deposited at the Cambridge Crystallographic data base: CCDC 976072 (2) 976383 (3), 976036 (6).

This material is available free of charge via the internet at <http://pubs.acs.org>. See DOI: 10.1039/c000000x/

1. S. Allard, M. Forster, B. Souharce, H. Thiem and U. Scherf, *Angewandte Chemie International Edition*, 2008, **47**, 4070-4098.
2. S. Sergeev, W. Pisula and Y. H. Geerts, *Chemical Society Reviews*, 2007, **36**, 1902-1929.
3. C. Li, M. Liu, N. G. Pschirer, M. Baumgarten and K. M  llen, *Chemistry Reviews* 2010, **110**, 6817-6855.
4. A. K. Geim and K. S. Novoselov, *Nature Materials*, 2007, **6**, 183-191.
5. M. J. Allen, V. C. Tung and R. B. Kaner, *Chemical Reviews*, 2009, **110**, 132-145.
6. K. S. Novoselov, V. I. Falko, L. Colombo, P. R. Gellert, M. G. Schwab and K. Kim, *Nature*, 2012, **490**, 192-200.
7. D. J. Roberts, D. Nolan, G. M. O M  ille, G. W. Watson, A. Singh, I. Ledoux-Rak and S. M. Draper, *Dalton Transactions*, 2012, **41**, 8850-8860.
8. M. Muller, C. Kubel and K. M  llen, *Chemistry, a European Journal*, 1998, **4**, 2099-2109.
9. L. Chen, Y. Hernandez, X. Feng and K. M  llen, *Angewandte Chemie International Edition*, 2012, **51**, 7640-7654.
10. M. Takase, T. Narita, W. Fujita, M. S. Asano, T. Nishinaga, H. Bente, K. Yoza and K. Mullen, *Journal of the American Chemistry Society*, 2013, **135**, 8031-8040.
11. R. Rieger and K. M  llen, *Journal of Physical Organic Chemistry*, 2010, **23**, 315-325.
12. R. Yamaguchi, S. Ito, B. S. Lee, S. Hiroto, D. Kim and H. Shinokubo, *Chemistry, an Asian Journal*, 2013, **8**, 178-190.
13. D. J. Jones, B. Purushothaman, S. Ji, A. B. Holmes and W. W. H. Wong, *Chemical Communications*, 2012, **48**, 8066-8068.
14. D. J. Gregg, C. M. A. Ollagnier, C. M. Fitchett and S. M. Draper, *Chemistry, a European Journal*, 2006, **12**, 3043-3052.
15. X. Li, X. Wang, L. Zhang, S. Lee and H. Dai, *Science*, 2008, **319**, 1229-1232.
16. C. Berger, Z. Song, X. Li, X. Wu, N. Brown, C. Naud, D. Mayou, T. Li, J. Hass, A. N. Marchenkov, E. H. Conrad, P. N. First and H. W. A. de, *Science*, 2006, **312**, 1191-1196.
17. S. M. Draper, D. J. Gregg and R. Madathil, *Journal of the American Chemistry Society*, 2002, **124**, 3486-3487.
18. D. J. Gregg, E. Bothe, P. Hofer, P. Passaniti and S. M. Draper, *Inorganic Chemistry*, 2005, **44**, 5654-5660.
19. A. Graczyk, F. A. Murphy, D. Nolan, V. Fernandez-Moreira, N. J. Lundin, C. M. Fitchett and S. M. Draper, *Dalton Transactions*, 2012, **41**, 7746-7754.
20. P. Rempala, J. Kroulik and B. T. King, *Journal of Organic Chemistry*, 2006, **71**, 5067-5081.
21. B. T. King, J. Kroulik, C. R. Robertson, P. Rempala, C. L. Hilton, J. D. Korinek and L. M. Gortari, *Journal of Organic Chemistry*, 2007, **72**, 2279-2288.
22. Z. Wang, F. Doetz, V. Enkelmann and K. M  llen, *Angewandte Chemie International Edition*, 2005, **44**, 1247-1250.
23. P. T. Herwig, V. Enkelmann, O. Schmelz and K. M  llen, *Chemistry, a European Journal*, 2000, **6**, 1834-1839.
24. S. M. Draper, D. J. Gregg, E. R. Schofield, W. R. Browne, M. Duati, J. G. Vos and P. Passaniti, *Journal of the American Chemistry Society*, 2004, **126**, 8694-8701.
25. C. J. Martin, B. Gil, S. D. Perera and S. M. Draper, *Chemistry Communications*, 2011, **47**, 3616-3618.
26. A. Graczyk, F. A. Murphy, D. Nolan, V. Fernandez-Moreira, N. J. Lundin, C. M. Fitchett and S. M. Draper, *Dalton Transactions*, 2012, **41**, 7746-7754.
27. E. Clar, *Polycyclic Hydrocarbons. Vol. 2*, Academic Press, 1964.
28. W. Hendel, Z. H. Khan and W. Schmidt, *Tetrahedron*, 1986, **42**, 1127-1134.
29. C. Bronner, S. Stremlau, M. Gille, F. Brau  e, A. Haase, S. Hecht and P. Tegeder, *Angewandte Chemie International Edition*, 2013, **52**, 4422-4425.